

DEVELOPMENT, CHARACTERIZATION AND EVALUATION OF ENTRECTINIB NANOSPONGES LOADED TABLETS FOR ORAL DELIVERY

MAMATHA PALANATI , D. V. R. N. BHIKSHAPATHI* 

Bir Tikandrajit University, Canchipur, Imphal West-795003, Manipur, India
*Corresponding author: D. V. R. N. Bhikshapathi; *Email: dbpati71@gmail.com

Received: 02 Aug 2023, Revised and Accepted: 09 Oct 2023

ABSTRACT

Objective: As Entrectinib is a lipophilic, basic, moderately permeable molecule with strongly pH-dependent solubility with antitumor activity in advanced and metastatic solid tumors, the current study was designed to improve the oral solubility of Entrectinib through incorporation into nanosponges tablets (NSs).

Methods: Box-Behnken Design was used to optimize the independent variables of β -Cyclodextrin (β -CD) NSs formation. β -CD NSs were prepared by an ultrasound-assisted method using diphenyl carbonate as cross-linking agent, which were later characterized and formulated into tablets by wet granulation method. The prepared tablets were evaluated for the physico-chemical properties and *in vitro* release of the drug.

Results: A series of fifteen experiments were performed based on the experimental runs generated from a three-factor, three-level Box-Behnken design (BBD). The range of mean particle size was 149-294 nm, the range for encapsulation efficiency % was 65.4%-87.3%, and the value for polydispersity index was 0.437. The zeta potential for the optimized formulation was found to be 38.1 Mv. The drug and excipients were compatibles as confirmed by Fourier Transformed Infrared (FTIR) Spectroscopy and Differential Scanning Calorimetry (DSC) studies. Scanning Electron Microscopic (SEM) analysis confirmed that the Entrectinib has successfully entrapped in the core of polymer. *In vitro* release of the Entrectinib-loaded NSs tablets (six compositions) were compared with a marketed product and satisfactory results were obtained. It was observed that rapid dissolution occurred in 0.1 N HCl for first 2 h (15.64 \pm 1.52% vs. 12.67 \pm 1.89%) and 98.94 \pm 2.43% of drug release was observed in Entrectinib loaded NSs and 91.78 \pm 1.37% in marketed product in 24 h. The prepared formulations were stable during 6 mo stability study period.

Conclusion: The study results studies of Entrectinib NS tablets indicated rapid dissolution due to changed solubility properties of the drug, compared to pure drug meeting the set objective of enhanced absorption. The formulated Entrectinib-loaded NSs can be beneficial in the treatment of cancers.

Keywords: Entrectinib, Cancer, Box-behnken design, Nanosponges, Tablets

© 2023 The Authors. Published by Innovare Academic Sciences Pvt Ltd. This is an open access article under the CC BY license (<https://creativecommons.org/licenses/by/4.0/>) DOI: <https://dx.doi.org/10.22159/ijap.2023v15i6.49022>. Journal homepage: <https://innovareacademics.in/journals/index.php/ijap>

INTRODUCTION

Entrectinib is a central nervous systems (CNS) active, shown to have antitumor activity in advanced and metastatic solid tumors by inhibiting tyrosine receptor kinases (TRK) A, B, and C, tyrosine kinase ROS proto-oncogene 1 (reactive oxygen species; ROS1), and anaplastic lymphoma kinase (ALK) [1, 2]. Entrectinib received its first global approval in Japan for the treatment of advanced or recurrent solid tumors, whereas the U. S. Food and Drug Administration approved for the treatment of adults with lung cancer and granted accelerated approval for the treatment of adult and pediatric patients with neurotrophic TRK fusion-positive solid tumors [3].

Entrectinib is a lipophilic, basic, moderately permeable molecule with strongly pH-dependent solubility [4]. It is a crystalline solid and is a Biopharmaceutical classification system (BCS) class II chemical with limited solubility and intermediate permeability. Entrectinib has a solubility of 40 mg/ml in 0.07 M HCl (pH 1.2), 0.03 mg/ml at pH 5.4, and 0.002 mg/ml at pH 6.4. Its solubility is much greater in the fed condition than in the fasted state. Peak plasma concentrations were discovered to be 2-4 h in the fasted condition versus 5-7 h in the fed state [5, 6]. It is critical to develop an alternate Entrectinib formulation with enhanced features in order to increase intrinsic solubility and decrease pharmacokinetic variability associated with existing capsule formulations.

Various formulation strategies have been used in recent years to improve the oral bioavailability of poorly soluble medicines. To boost oral bioavailability, various classical approaches such as complexation, co-solvency, salt formation, micronization, and the use of permeation enhancers have been tested [7]. All of these approaches, however, have proven limited efficacy in drug delivery. Among the different techniques, nano-based drug delivery systems

(NBDDS) have enormous potential to improve the bioavailability of poorly soluble medicines [8]. NBDDS have sparked a lot of research interest in recent years because of the potential benefits, such as improving lipophilic drug solubility, increasing permeability, improving drug stability, controlling drug distribution and elimination, and targeting drug delivery to a specific site. Several NBDDS have been produced, including nanocrystals, nanoemulsions, nanosponges (NSs), nanobubbles, liposomes, polymeric micelles, polymeric nanoparticles, and inorganic nanocarriers [9, 10].

Many studies have shown that NS dosage forms can increase the solubility and, thus oral bioavailability of poorly soluble medicines [11]. They shield molecular compounds from degradation and these have high selectivity, biocompatibility, degradability, and extended-release behaviour which are used in cancer therapy [12]. The sponge functions as a three-dimensional scaffold or network. Polyester is used for the backbone. To produce the polymer, it is combined in solution with cross-linkers. The end result is spherically shaped particles with cavities where drug molecules can be housed [13]. Because polyester is biodegradable, it degrades gradually in the body. Its drug payload is released in a predictable manner as it degrades. By adjusting the amounts of crosslinker to polymer, the NSs can be synthesized to be a certain size and to release medications over time. For oral administration, these may be dispersed in a matrix of excipients, diluents, lubricants, and anti-caking agents suitable for the preparation of tablets or capsules, and the major advantages of these capsules or tablets are reduced total dose, retention of dosage form, reduced toxicity, and improved patient compliance through prolonged release [14].

Utilizing Design of Experiments is an innovative advance in optimizing and transmitting experimental factors. Simple experimental plans and statistical tools for information analysis can offer a huge advantage regarding the system under examination

after a small number of experiments [15]. A statistical technique called Response Surface Methodology is utilized for DoE and the construction of experimental models that link several interacting components [16]. Box-Behnken designs (BBD) are the two most often utilized designs in response surface modeling [17].

The aim of this study was to improve the oral solubility of Entrectinib through incorporation into NSs. The study included optimization of the parameters for preparation of Entrectinib loaded NSs, characterization and evaluation of Entrectinib loaded NSs tablets.

MATERIALS AND METHODS

Materials

Entrectinib was obtained from Hetero Drugs Pvt Ltd, Hyderabad. ROZLYTREK was acquired from South Delhi Pharma, Delhi, India. β -Cyclodextrin was from Gangwal Chemicals Pvt. Ltd. Mumbai, India; diphenyl carbonate was from Euclid Pharmaceuticals Limited, Mumbai, and dimethyl formamide, ethanol and methanol were obtained from Qualigens, Thermo Fisher Scientific India Ltd, Mumbai. Gelatin, HPMC K4M, lactose monohydrate, and magnesium stearate were obtained from SD Fine chemicals, Hyderabad.

Formulation development

Preparation of β -cyclodextrin NSs

β -Cyclodextrin (β -CD; polymer) based NSs were prepared in our laboratory by using diphenyl carbonate (DPC) as a cross-linking by ultrasound assisted method at a composition of 1:6 (β -CD: DPC) [18]. In a 250 ml flask, required quantity of anhydrous β -CD was dissolved in dimethyl formamide. DPC was added to this reaction mixture and refluxed in an oil bath (NSW 199, Narang Scientific Works Private Limited, New Delhi) at 90 °C for 6 h under stirring. After completion of the reaction, the obtained product was washed with water and subsequently purified by Soxhlet extraction with

ethanol up to 6 h. The white powder thus obtained was dried overnight in an oven at 60 °C and subsequently ground in a mortar. The fine powder obtained was re-dispersed in water [19]. The colloidal part that remained suspended in water was recovered by lyophilization (Lark Innovative Fine Technologies Lyophiliser, India).

Fabrication of entrectinib-loaded β -CD NSs

Entrectinib-loaded NSs were prepared by lyophilization technique. 500 mg of NSs were suspended in 100 ml of MilliQ water using a mechanical stirrer (RQ 121-D, Remi India). To the above mixture, 600 mg of Entrectinib was added and the mixture was sonicated (ENUP 750, Remi India) for 20 min to prevent aggregation. Then this mixture was kept under continuous stirring for specified time period. To separate the uncomplexed drug, the suspensions were centrifuged (Micro III, Remi India) at 2000 rpm for 20 min. The colloidal supernatant was separated and freeze-dried using a lyophilizer at a temperature of -20 °C and pressure of 13.33 mbar. After lyophilization the collected dry powder was stored in a desiccator [20].

Experimental design

Box-behnken design

A three-factor, three-level BBD was used to explore and optimize the main effects, interaction effects, and quadratic effects of the formulation ingredients on the performance of the NSs. This design is suitable for exploring quadratic response surfaces and constructing second-order polynomial models [21]. Based on the boundary of the NSs domain, independent or formulation variables (Molar ratio of polymer to cross-linker; X_1 , Stirring speed; X_2 , and Stirring time; X_3) were identified as shown in table 1. The significant response factors used to assess the quality of the NS formulation including mean particle size (PS; Y_1), entrapment efficiency (EE; Y_2), and Polydispersity Index (PI; Y_3) (table 1 and 2).

Table 1: List of dependent and independent variables in box-behnken design

Independent variables		Levels			
Variable	Name	Units	Low (-1)	Middle (0)	High (+1)
X_1	Molar ratio of polymer to cross-linker		0.2	0.4	0.6
X_2	Stirring Speed	rpm	2000	3000	4000
X_3	Stirring time	mins	300	450	600
Dependent variable		Goal			
Y_1	Mean Particle size	nm	Minimize		
Y_2	Entrapment Efficiency	%	Maximize		
Y_3	Polydispersity Index		Maximize		

The BBD nanosponges was generated using Design Expert® software (Version 7.0, Stat-Ease Inc., Silicon Valley, CA, USA), and the data obtained were analyzed by the same software. All responses were fitted to a second-order quadratic model by the Design Expert software. The second-order quadratic or polynomial equation can be approximated in the following mathematical model:

$$Y = \beta_0 + \beta_1 X_1 + \beta_2 X_2 + \beta_3 X_3 + \beta_4 X_1 X_2 + \beta_5 X_2 X_3 + \beta_6 X_1 X_3 + \beta_7 X_1^2 + \beta_8 X_2^2 + \beta_9 X_3^2$$

Where Y is the level of the measured response, β_0 is the intercept, β_1 to β_9 are the regression coefficients, X_1 , X_2 , and X_3 stand for the main effects, $X_1 X_2$, $X_2 X_3$, and $X_1 X_3$ represents the interaction between the main effects, X_1^2 , X_2^2 and X_3^2 are the quadratic terms of the independent variables that were used to simulate the curvature of the designed sample space. A backward elimination procedure was adopted to fit the data to the quadratic model. The model adequacy was verified by analysis of variance (ANOVA), lack-of-fit and multiple correlation coefficient (R^2) tests provided by the Design Expert software. The value of coefficients reflected the effect of independent variables and their interaction on the dependent variables. A positive coefficient indicates a synergistic effect; meanwhile, a negative one reflects an antagonistic effect. The significance of individual coefficients was determined by ANOVA

test, and one was considered significant if the p-value was <0.05. The quadratic models generated from the regression analysis were used to construct the 3-dimensional graphs, in which the response parameter Y was represented by a curvature surface as a function of X. The effects of independent variables on the response parameters were visualized from the perturbation plots and 3D contour plots. Further optimization was conducted with a desirability function.

Optimization

The optimal points for the independent variables were attained using numerical optimization technique by setting restrictions on the response parameters and influencing factors. The NSs formulation was prepared in triplicate under optimal conditions to verify the validity optimization technique.

Characterization of prepared entrectinib NSs

Particle size, polydispersity index and zeta potential

The PS distribution of Entrectinib NSs was observed by dynamic light scattering method. The measurements were made at fixed angle of 90° for all samples. The samples were suitably diluted with Milli Q water before measurement. The mean hydrodynamic diameter (Dh) and PI of the particles were calculated using cumulated analysis after averaging

three measurements. ZP measurements were also made using an additional electrode in the same instrument (Mastersizer2000, Malvern

Instruments Ltd, Worcestershire, UK). All the experiments were conducted in triplicate at 25±2 °C [22].

Table 2: Composition of entrectinib nanosponges formulation by box behnken design

F. No	Variables 1 X1: Molar ratio polymer to cross linker mg	Variables 2 X2: Stirring speed (rpm)	Variables 3 X3: Stirring time (min)	Response 1 Y1: Mean particle size (nm)	Response 2 Y2: Encapsulation efficiency (%)	Response 3 Y3: PI
EF1	0.2	2000	450	294	65.4	0.271
EF2	0.6	2000	450	198	81.2	0.377
EF3	0.2	4000	450	271	67.6	0.263
EF4	0.4	4000	600	243	78.6	0.369
EF5	0.2	3000	300	287	69.2	0.275
EF6	0.6	3000	300	194	82.9	0.385
EF7	0.2	3000	600	266	66.7	0.296
EF8	0.6	3000	600	189	83.6	0.398
EF9	0.4	2000	300	248	74.1	0.392
EF10	0.4	4000	300	235	76.8	0.380
EF11	0.2	2000	600	265	70.5	0.265
EF12	0.6	4000	450	149	87.3	0.437
EF13	0.4	3000	450	261	79.5	0.367
EF14	0.4	3000	450	256	73.2	0.375
EF15	0.2	3000	450	272	68.6	0.269

Encapsulation efficiency (%)

EE is the ratio of weight of drug entrapped into a carrier system to the total drug added. Drug loading is the ratio of drug to the weight of total carrier system. Weighed amount of Entrectinib-loaded NSs complex was dissolved in methanol, sonicated for 10 min to break the complex, diluted suitably, and then analysed by UV spectrophotometer (Lab India UV-3000+, Lab India instruments Pvt. Ltd.) at 262 nm to determine the amount of Entrectinib present in the formulation [18]. The percent drug encapsulation efficiency was calculated using the following equation:

$$\text{Encapsulation efficiency (\%)} = \frac{\text{Amount of drug after filtration}}{\text{Total amount of drug in the sample}} \times 100$$

Scanning electron microscopy (SEM)

The morphology of the plain NSs and Entrectinib-loaded NSs was observed under SEM. One drop of diluted NSs suspension was deposited on a film-coated copper grid and stained with one drop of 2% (w/v) aqueous solution of phosphotungstic acid and then allowed to dry for contrast enhancement [23]. The samples were examined at a magnification of 45000× by Transmission Electron Microscopy (TEM; JEM-2000 EXII; JEOL, Tokyo, Japan).

Fourier-transformed infrared (FTIR) spectroscopy

The FTIR spectra of β-CD, plain NSs, Entrectinib, physical mixture and Entrectinib loaded NSs were carried out by potassium bromide disc method using Tensor 27 FTIR Spectrophotometer in the region of 4000 to 600 cm⁻¹ (Tensor 27, Bruker Optics, Germany) [19].

Differential scanning calorimetry (DSC)

DSC of β-CD, plain NSs, Entrectinib, physical mixture and Entrectinib loaded NSs were carried out using a Perkin Elmer DSC/7 differential scanning calorimeter (Perkin-Elmer, CT-USA) equipped with a TAC 7/DX instrument controller. The instrument was calibrated with indium for melting point and heat of fusion. A heating rate of 10 °C/min was employed in the 30-400 °C temperature range. Standard aluminium sample pans (Perkin-Elmer) were used; an empty pan was used as the reference standard. Analyses were performed in triplicate on 5 mg samples under nitrogen purge [23].

Preparation of entrectinib-loaded NSs tablets

The oral formulation of Entrectinib-loaded NSs were prepared by wet granulation method. The binding agent's gelatin and the polymer hydroxy propyl methyl cellulose (HPMC K4M; 100 mg) were used to prolong the drug release up to 24 h. An accurately weighed quantity of Entrectinib loaded NSs corresponding to 200 mg Entrectinib was mixed for 10 min in mortar and pestle with the required quantity of lactose

monohydrate to attain 500 mg tablet. Then, granules were prepared using different binder solutions. After granulation and drying, magnesium stearate was added and blended for another 2 min. Then 25 mm diameter round tablets were prepared using a single punch tablet machine with flat-faced single punch (Tablet Compression Machine-Single Punch, Harrisons Pharma Machinery Private Limited) [24].

Evaluation of tablet formulation

Uniformity of weight

Twenty tablets were selected at random, individually weighed in a single pan electronic balance and the average weight was calculated. The uniformity of weight was determined according to the specifications of British Pharmacopoeia (BP 2013).

Drug content

The Entrectinib content of the prepared tablets was carried out according to the method mentioned previously. The triturated tablets were treated with ethanol for the extraction of drug from NSs. The sample was suitably diluted and drug content was estimated using UV spectrophotometer [25, 26].

Hardness test

Hardness of the prepared tablets was measured using the tablet hardness tester (Monsanto). Three tablets were selected for testing and results were expressed in kg/cm².

Friability test

Friability test was done in a digital tablet friability tester apparatus, where the tablets were subjected to the combined effect of abrasion and shock by utilizing a plastic chamber that revolves at 25 rpm, while dropping the tablets at a distance of six inches with each revolution. Pre-weighed samples of 20 tablets were placed in the friability chamber, which was operated for 100 revolutions. At the end of the rotation, the tablets were removed from the drum, carefully brushed to free them from adhering dust and reweighed. Conventional compressed tablets lose less than 0.5-1.0% of their weight, which is generally considered acceptable [26, 27].

The percent friability is given by the equation:

$$\% \text{ Friability} = \frac{W1 - W2}{W1} \times 100$$

Where W0 is the weight of the tablets before the test and W is the weight of the tablets after test.

In vitro release study of entrectinib NSs

Drug release was determined by dialysis method; 2 ml of each formulation (test and control) were poured into dialysis bags and put

into 25 ml phosphate buffer (pH 7.4) and stirred (100 rpm at room temperature). At predetermined time intervals, 2 ml of phosphate buffer was taken and then substituted by fresh phosphate buffer. Finally, the amounts of released Entrectinib in phosphate buffer were measured by spectrophotometer at 262 nm. Aliquots withdrawn were assayed at each time interval for the drug released at λ_{\max} of 262 nm using UV-Visible spectrophotometer by keeping phosphate buffer pH 7.4 as blank and the amount of released drug was estimated [28].

In vitro release study of entrectinib-loaded tablets

In vitro release of drug from Entrectinib loaded tablets and pure drug was performed using the type II USP dissolution apparatus. The dissolution medium was 900 ml 0.1 N HCl for first 2 h then replaced with phosphate buffer pH 6.8 at a speed of 50 rpm and a temperature of 37 ± 0.5 °C. The samples were withdrawn at 0, 1, 2, 4, 8, 12, 16, 20, and 24 h. Equal amount of the fresh dissolution medium, retained at the same temperature, was immediately replaced. The samples were suitably diluted and analysed using UV-spectrophotometer at 262 nm. The dissolution experiments were conducted in triplicate and the results were compared with marketed product [29].

Drug release kinetics

Confirmation of the method of drug release and its approach from the *in vitro* release study was performed by integrating into kinetic models (zero order, 1st order, Higuchi's and Korsmeyer Peppas's model). CAP release through micelle formulation was understood by the curve fitting technique [30]. Results obtained through *in vitro* release studies were verified with different kinetic equations [31].

Stability studies

Among all batches of Entrectinib-loaded NSs were subjected to immutability studies in accordance with guidelines of ICH stability protocol. The test specifications include temperature of 40 ± 2 °C and relative humidity of $75 \pm 5\%$ RH for a time period of 6 mo in Humidity chamber (REMI, Mumbai) [32]. The specifications to be evaluated in the stability study period include PS, EE, *in vitro* drug released, and drug content.

RESULTS AND DISCUSSION

Preparation of entrectinib-loaded NSs

Over the last decade, numerous efforts have been directed to the method of preparation and application of NSs. Among the numerous types of NSs, β -CD-based NSs have gotten the most attention and are being investigated the most [33].

β -CD NSs can form complexes with different types of lipophilic or hydrophilic molecules. The release of the entrapped molecules can be varied by modifying the structure to achieve prolonged release kinetics or a faster release. They offer unique advantage of controlled release and are biologically safe and biodegradable material [34]. NSs have been synthesized by substituting hydrogen of the primary hydroxyl groups present on the outer cavity of the parent β -CD unit. Thus, the drug molecules could be included inside the nanocavities and due to the cross-linking, further interactions of the guest molecules with more β -CD units might be thought. Moreover, the presence of the cross-linked network might also form Nano channels in the NSs structure for the polymer mesh. This peculiar structural organization might be responsible for the increased solubilisation and protection capacities of NSs [35]. The prepared NSs were loaded with freeze drying method as lyophilization is a suitable process in improving stability of NSs. In general, a good lyophilizate maintains the physical and chemical properties of the prime product [36].

Experimental design

Through preliminary screening the molar ratio polymer to crosslinker, stirring speed and stirring time were identified as the most significant variables affecting the performance parameters like mean PS, % EE and PDI of Entrectinib NSs. These independent variables were initially examined by varying the level of one at a time in order to determine the variable range. From the trials, the molar ratio polymer to crosslinker (0.2-0.6), stirring Speed (2000-4000 rpm) and stirring time (300-600) were identified. Based on the initial results, a BBD was employed to optimize the influencing variables. A series of experiments were performed based on the experimental runs generated from a three-factor, three-level BBD. The range of mean PS (Y_1) for all batches was 149–294 nm, the range for % EE (Y_2) was 65.4%–87.3%, and the range for PDI (Y_3) was 0.263–0.437. All responses were fitted to a second quadratic model and the adequacy of this model was verified by ANOVA, tests provided by Design-Expert software.

Particle size

PS determination is an important quality control measure to measure the ability of any NSs formulation. PS is a critical value for NSs; smaller PS provides a larger interfacial surface area for drug absorption. In addition, a smaller PS may permit a faster release rate [37]. The mean particle size of the NSs was found to be in the range of 149-294 nm. The polynomial model shown that all the variables (X_1 , X_2 and X_3) have a significant effect. The observed values are in close agreement with the predicted values, as shown in fig. 1.

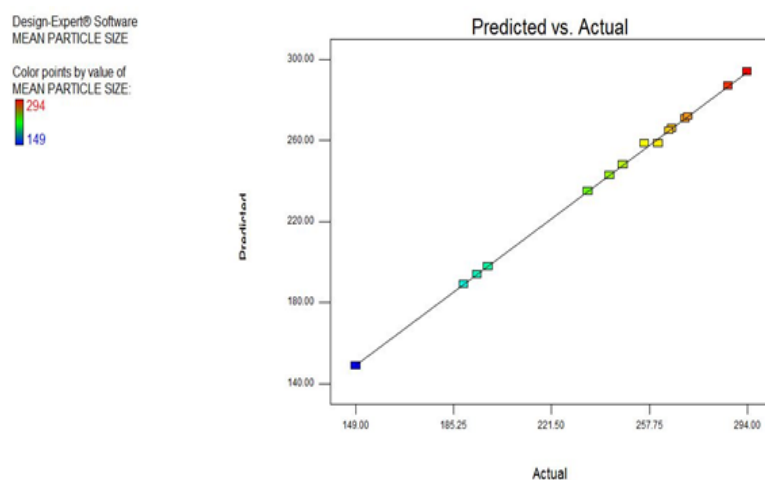


Fig. 1: Comparison between predicted and actual values of mean particle size

The mathematical model generated for mean PS (Y_1) was found to be significant with F-value of 0.0442 implies the model is significant.

There is only a 0.02% chance that a "Model F-Value" this large could occur due to noise. The quadratic term have significant effects on the

PS, since the *P* values less than 0.05 represent the significant model terms. The influence of the main and interactive effects of independent variables on the PS was further elucidated using the perturbation, contour and, 3D response surface plots. The relationship between the dependent and independent variables was further elucidated using 3D response surface plots and corresponding contour plots. The

interaction between A and B on mean particle size at a fixed level of C is shown in fig. 2(a). The respective contour plots are as shown in fig. 2(b). As the stirring speed increases the particle size was decreased. Likewise, as the stirring time increases the particle size reduced. Particle size was decreased as the Molar ratio polymer to cross-linker was increased as shown in fig. 2(c).

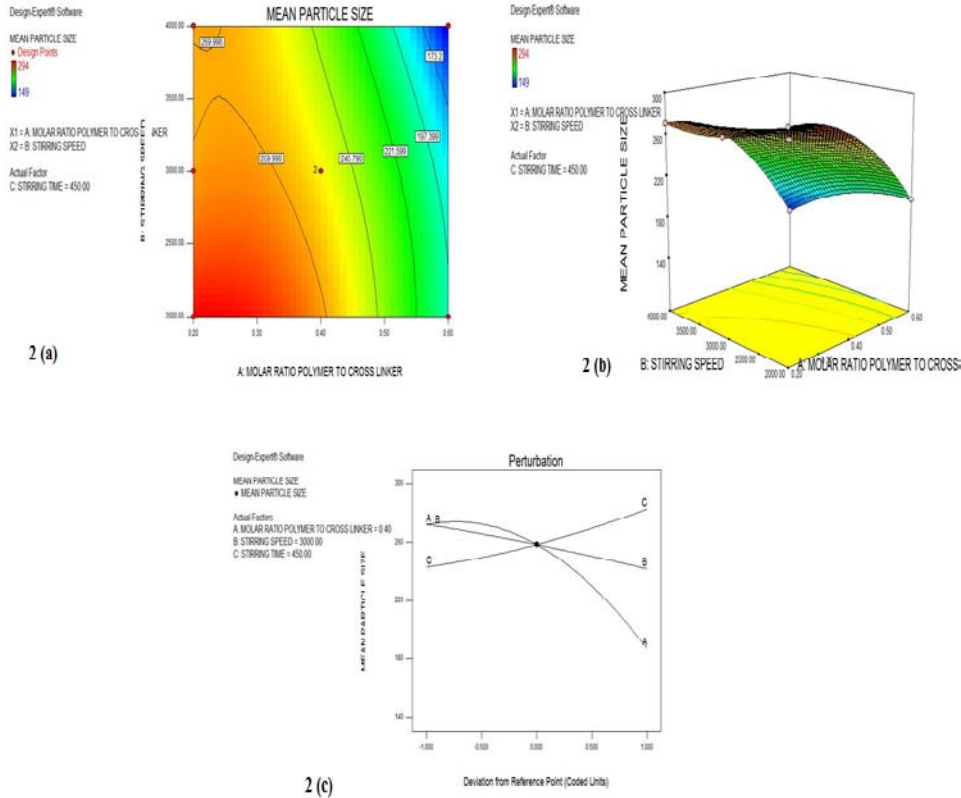


Fig. 2 (a): Contour plot showing the influence of molar ratio polymer to cross-linker, stirring time, and stirring speed on mean particle size fixed level of C; 2 (b): 3D-Contour Plot showing the influence of molar ratio polymer to cross-linker, stirring time, and stirring speed on mean particle size fixed level of C; 2 (c): Two-dimensional perturbation plot showing the influence of molar ratio polymer to cross-linker, stirring time, and stirring speed on mean particle size fixed level of C

Entrapment efficiency (%)

Drug encapsulation is significant for improving the solubility and bioavailability of the drug [38]. The EE of the NSs was found to be in

the range of 65.4% to 87.3%. The polynomial model shown that all the variables (X_1 , X_2 and X_3) have a significant effect. The observed values are in close agreement with the predicted values, as shown in fig. 3.

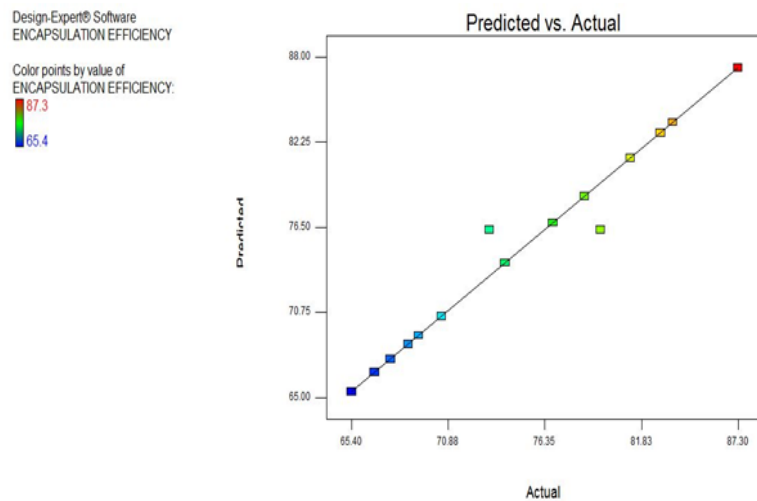


Fig. 3: Comparison between predicted and actual values of entrapment efficiency (%)

The mathematical model generated for EE (Y_2) was found to be significant with an F-value of 0.0255, which implies the model is significant. The "Lack of Fit F-value" of 0.0162 implies the Lack of Fit is significant relative to the pure error. There is a 1.78 % chance that a "Lack of Fit F-value" this large could occur due to noise. Results of the equation indicate that the effect of X_1 is more significant than X_2 and X_3 . The factorial equation for EE showed a good correlation coefficient (0.9992). The influence of the main and interactive effects

of independent variables on the EE was further elucidated using the perturbation and contour plots. The relationship between the dependent and independent variables was further elucidated using 3D response surface plots and corresponding contour plots. The interaction between X_1 and X_2 on EE at a fixed level of C is shown in fig. 4(a). The respective contour plots are as shown in fig. 4(b). As the stirring speed increased the EE was increased, whereas the volume of solvent had an antagonistic effect on EE.

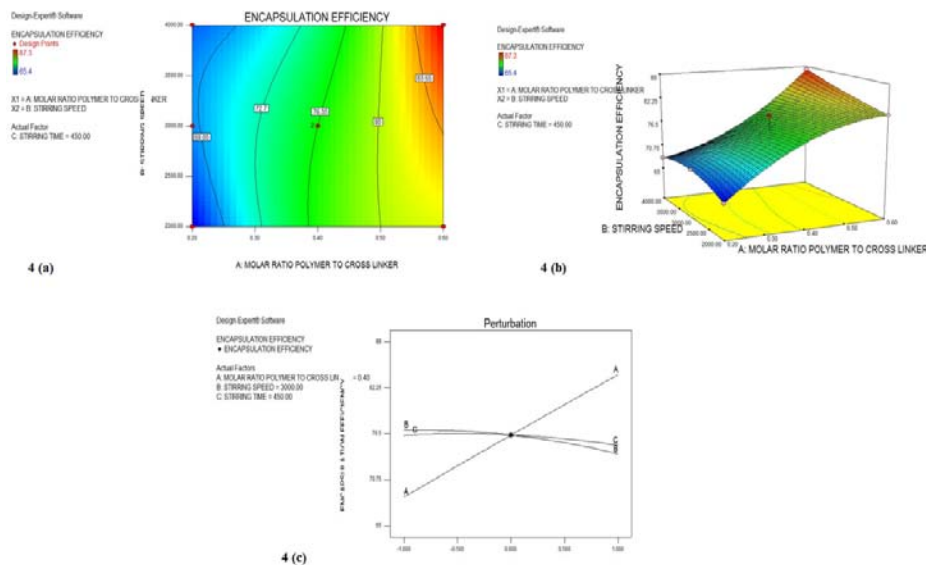


Fig. 4(a): Contour plot showing the influence of molar ratio polymer to cross linker, stirring time, and stirring speed on EE fixed level of C; 4(b): 3D-Contour Plot showing the influence of molar ratio polymer to cross linker, stirring time, and stirring speed on EE fixed level of C; 4(c): Two-dimensional Perturbation plot showing the influence of molar ratio polymer to cross linker, stirring time, and stirring speed on EE fixed level of C

Polydispersity index

PDI is a measure of the range of size distribution. Values greater than 1 indicate that the distribution is poly-dispersed. PDI value was found to be 0.437. PDI is significant in terms of stability,

solubility, dissolution and permeation through various tumour tissues and organs [39]. The polynomial model shown that all the variables have a significant effect on PDI of drug-loaded NSs. The observed values are in close agreement with the predicted values as shown in fig. 5.

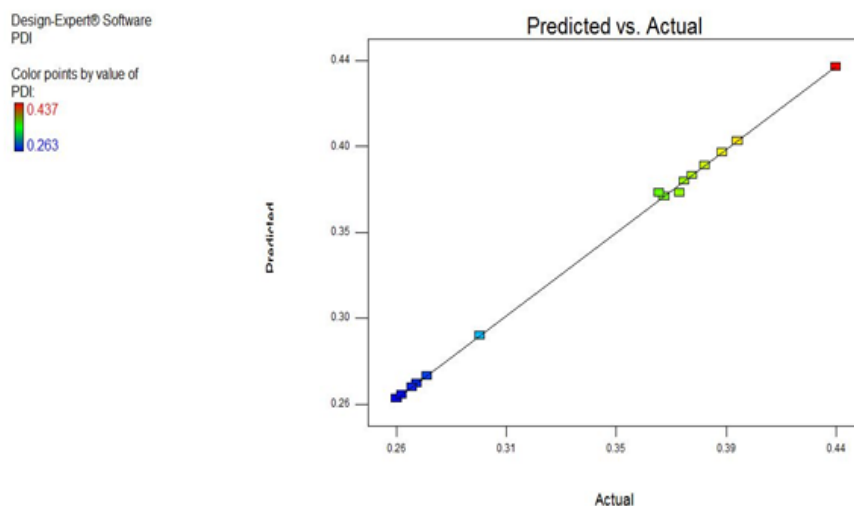


Fig. 5: Comparison between predicted and actual values of polydispersity index (PDI)

The mathematical model generated for PDI was found to be significant with F-value of 0.0234 implies the model is significant. There is only a 0.04% chance that a "Model F-Value" this large could

occur due to noise. The "Lack of Fit F-value" of 0.0165 implies the Lack of Fit is significant relative to the pure error. There is a 01.07% chance that a "Lack of Fit F-value" this large could occur due to

noise. The influence of the main and interactive effects of independent variables was further elucidated using the perturbation and contour plots. The interaction between X_1 and X_2 on PDI at a fixed level of C is shown in fig. 6(a). The respective contour plots are as shown in fig. 6(b, c). The increase in the PDI with a concomitant increase in the molar ratio polymer to cross-linker, stirring speed

and stirring time. This phenomenon may be explained by the fact that a higher proportion of molar ratio polymer to cross-linker gives optimized PDI. As the stirring speed increases the PDI was decreased. Likewise, as the stirring time increases the PDI reduced. PDI was decreased as the molar ratio polymer to cross-linker was increased.

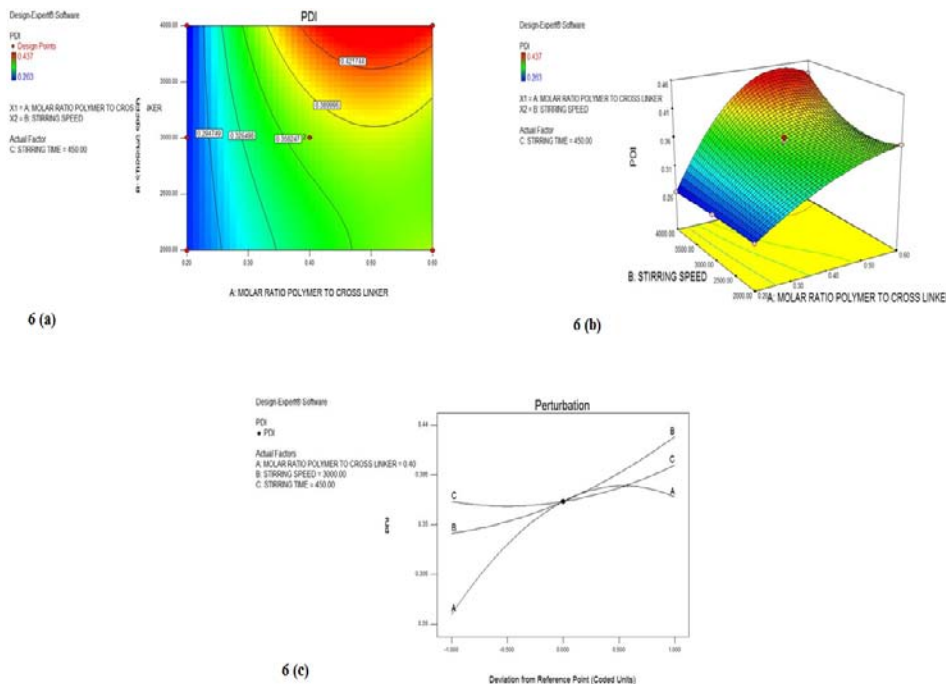


Fig. 6(a): Contour plot showing the influence of molar ratio polymer to cross linker, stirring time, and stirring speed on PDI fixed level of C; 6(b): 3D-Contour Plot showing the influence of molar ratio polymer to cross linker, stirring time, and stirring speed on PDI fixed level of C; 6(c): Two-dimensional Perturbation plot showing the influence of molar ratio polymer to cross linker, stirring time, and stirring speed on PDI fixed level of C

Characterization of prepared entrectinib NSs

Particle size, polydispersity index, zeta potential, and encapsulation efficiency

The mean PS of optimized formulation was found to be 149 nm and 294 nm (within nanometric range). PS is a critical value for NSs; smaller PS provides a larger interfacial surface area for drug absorption. In addition, a smaller PS may permit a faster release rate

[38]. PDI of optimized formulation was found out to be 0.437, indicating uniformity of particle size within formulation (fig. 7 and 8). PDI is significant in terms of stability, solubility, dissolution and permeation through various tumour tissues and organs [39]. The zeta potential study was done by zetasizer. The zeta potential for the optimized formulation was found to be 38.1Mv, which shows that the formulation is stable [40]. The EE of the NSs was found to be in the range of 65.4% to 87.3%.

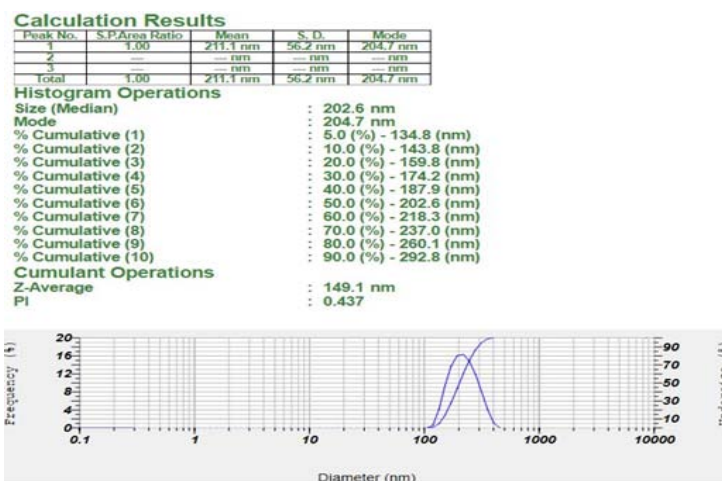


Fig. 7: Particle size distribution of entrectinib-loaded nanospheres

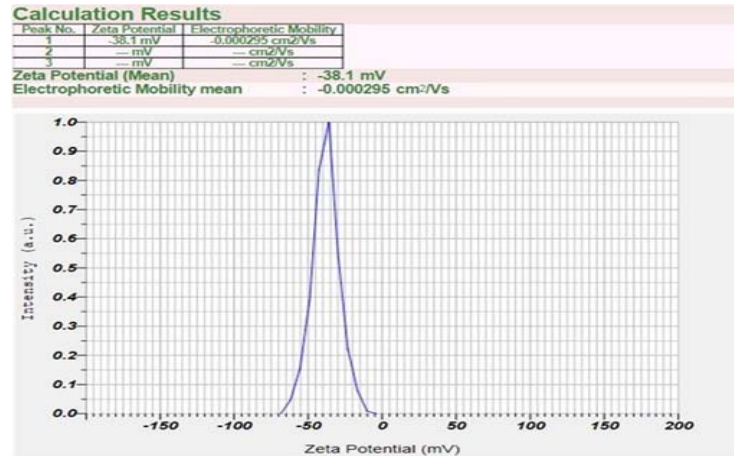


Fig. 8: Particle size distribution of entrectinibloaded nanosponges

Fourier-transformed infrared (FTIR) spectroscopy

FTIR spectra of Entrectinib (fig. 9), β -Cyclodextrin (fig. 10), Diphenyl carbonate (fig. 11) and physical mixture (fig. 12) are observed. The FTIR spectrum of physical mixture revealed that the functional

groups of Entrectinib, HPMC K4M and other excipients were seen without deviation [18]. Hence it was concluded that all excipients in the mixture were found to be compatible with each other and does not showed any interaction with each other.

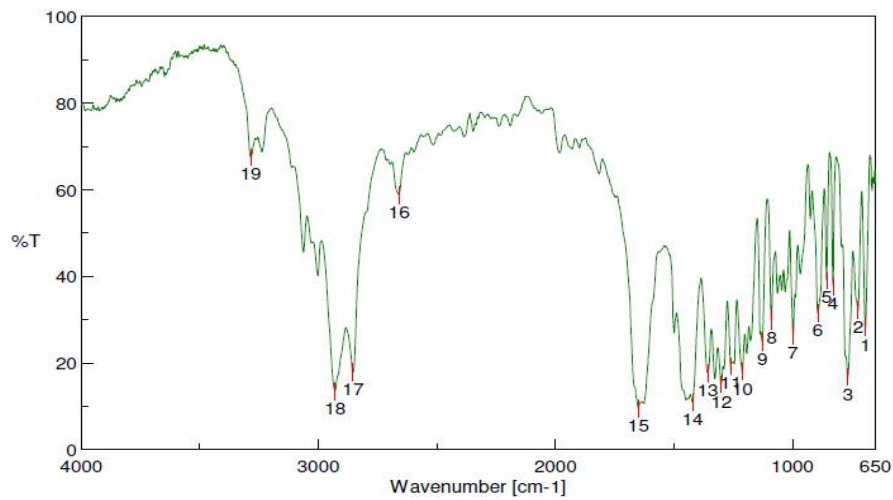


Fig. 9: FTIR spectra of entrectinib

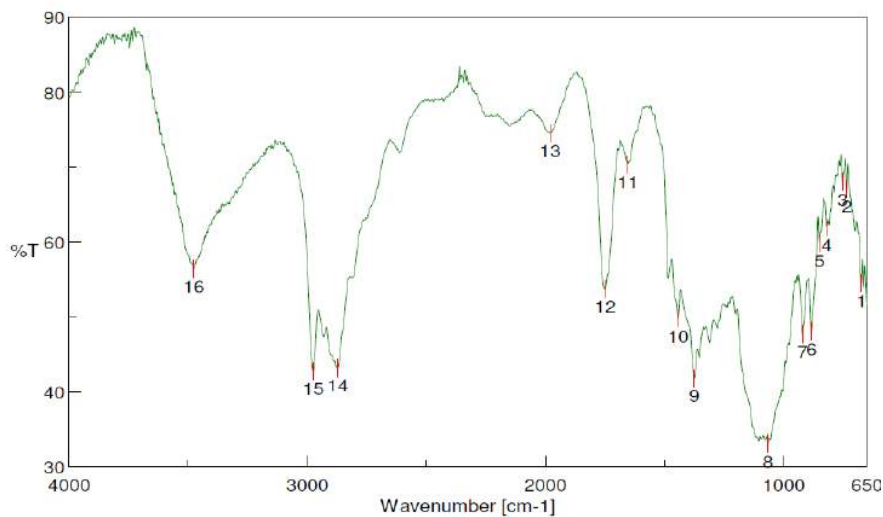


Fig. 10: FTIR spectra of β -cyclodextrin

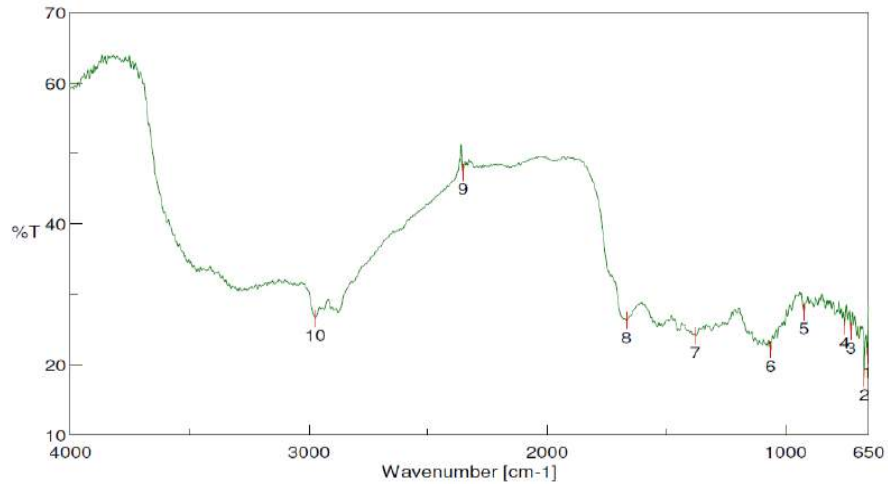


Fig. 11: FTIR spectra of diphenyl carbonate

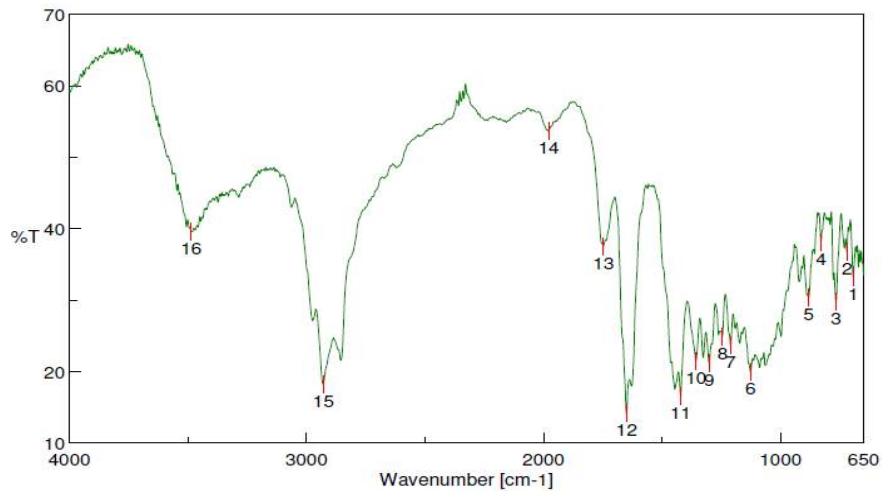


Fig. 12: FTIR Spectra of physical mixture

Differential scanning calorimetry (DSC)

The physical mixture of Entrectinib, β -CD and DPC showed sharp melting endotherm at an onset temperature of around 130-132 °C, a peak temperature of 142.57 °C and ends at the temperature of

around 150-152 °C [20]. Furthermore, it also slightly shows a glass transition at 216-218 °C may be corresponding to the melting. Thus, it indicates no interaction between the Entrectinib and excipients as shown in fig. 13 and 14.

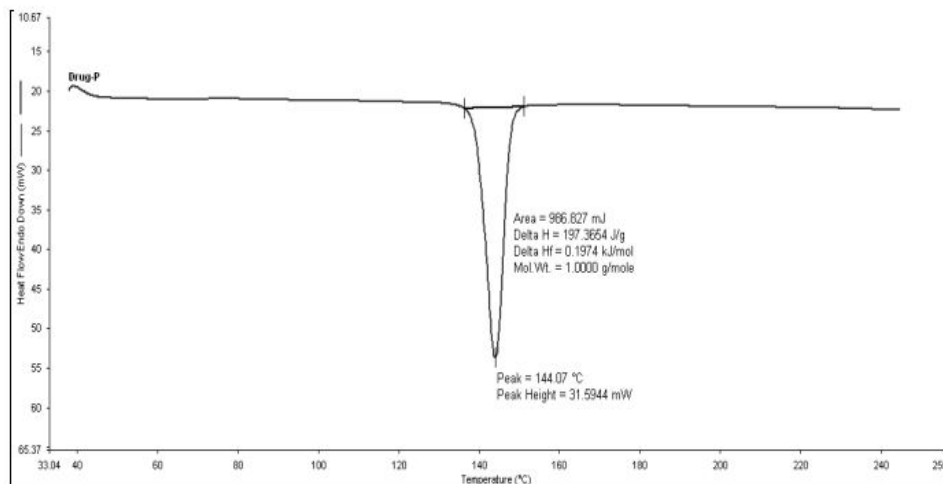


Fig. 13: DSC thermogram of pure entrectinib

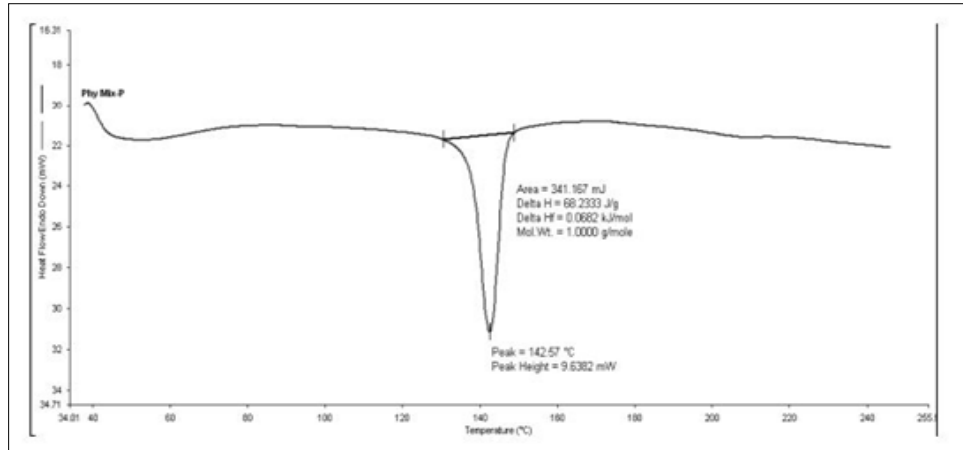
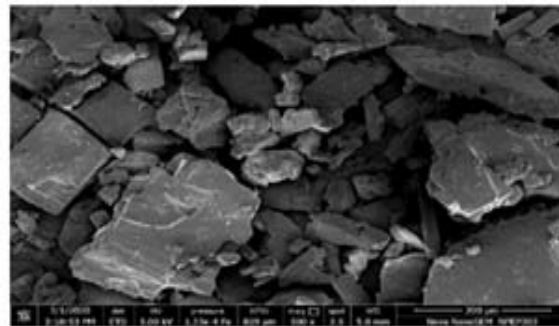


Fig. 14: DSC Thermogram of physical mixture

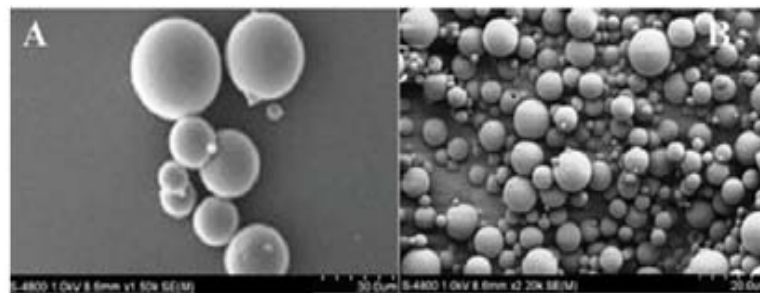
Scanning electron microscopy (SEM)

Surface topography of Entrectinib, β -CD, DPC and, Entrectinib loaded NSs were observed. SEM image of Entrectinib showed combination of sharp, prismatic, slender and flattened crystal habits with an average size range of $>30 \mu$, confirm the crystalline nature of

Entrectinib (fig. 15a). SEM image revealed that formulated Entrectinib NSs formulation was found to be highly porous structure and it revealed that the functional groups of drug, polymer, and cross-linker were detected in the sample. Thus, it was confirmed that the Entrectinib has successfully entrapped in the core of polymer as shown in fig. 15(b).



15 (a)



15 (b)

Fig. 15(a): SEM images of pure Entrectinib; 15(b) SEM micrograph of Entrectinib loaded NSs at magnification of 45000 \times

Stability studies

For six months, the storage stability of optimized Entrectinib-loaded NSs was investigated at test specifications of temperature of $40 \text{ }^\circ\text{C} \pm 2 \text{ }^\circ\text{C}$ and relative humidity of $75 \pm 5\%$ RH. Drug content, EE, *in vitro* drug release, and PS were measured at the 0th, 30th, 60th, 120th, and 180th day. No noteworthy alteration in drug quantity and PS was noted at days of storage. The EE hardly changed, signifying that NSs could shield Entrectinib from deterioration or degradation [45]. Furthermore, as storage time passed, the mean *in vitro* drug release pattern was also no changed [40]. The results indicated that the

prepared Entrectinib-loaded NSs were stable throughout the storage time and did not shown any leakage or drug degradation.

Evaluation of tablet formulation

Physico-chemical parameters evaluation

The weight and the thickness of Entrectinib-loaded NSs tablets were within the limits of uniformity. The weight was ranged from 500 ± 3.45 to 501 ± 6.73 . Thickness ranged between 5.1 ± 0.05 to 5.4 ± 0.15 mm. The drug content ranged from $98.11 \pm 1.63\%$ to $99.34 \pm 1.55\%$. The adequate tablet hardness is a necessary requisite

for consumer acceptance and handling. The measured hardness was ranged between 5.4 to 5.8 Kg/cm². The friability tests for all were done as per the standard procedure I. P. the results of the friability test. The data indicates that the friability was less than 1% in all formulations, ensuring that the tablets were mechanically stable [24, 25, 28].

In vitro release study of entrectinib NSs

The *in vitro* release profile of Entrectinib from Entrectinib NSs was compared to plain Entrectinib, as shown in fig. 16. The Entrectinib

release behavior from NSs suggested a sustained release for up to 60 min. The sustained release behavior from NSs accounted for the release of up to 98.41±1.63% vs. 4.79±1.19% by pure drug suspension over a time period of 1 h. The slow release of pure Entrectinib may be due to its hydrophobic nature and low aqueous solubility. It was evident that Entrectinib NSs had better release qualities than normal Entrectinib. This could be because NSs have the ability to improve the dissolution of poorly soluble drugs by trapping them inside their nanochannels and cavities, hiding their hydrophobic moieties and boosting their solubility [20, 22].

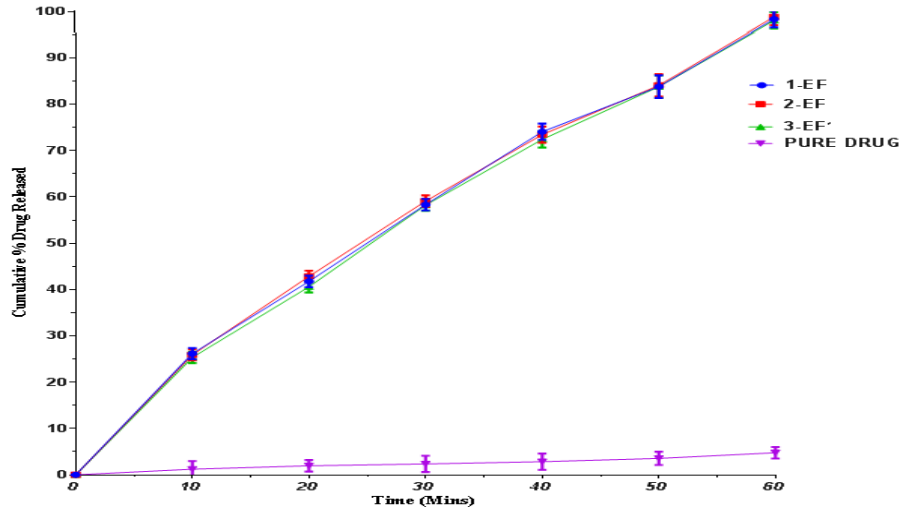


Fig. 16: *In vitro* release study of Entrectinib NSs (triplicate) in comparison with pure drug, (All determinations were performed in triplicate and values were expressed as mean±SD, n=3)

In vitro release study of entrectinib-loaded NSs tablets

The prepared Entrectinib-loaded NSs were compressed into 6 different compositions of tablets and further was evaluated for % cumulative drug release. It indicated rapid dissolution in 0.1 N HCl for first 2 h with 15.64±1.52% of drug released and its near to the comparator (12.67±1.89%), 98.94±2.43% of drug release was observed in Entrectinib loaded NSs and 91.78±1.37% in marketed product. The dissolution rate profile for the formulation in comparison to ROZLYTREK (marketed product) is presented in

the fig. 17. The fabricated NSs that comprised of complex networks of β -CD with a roughly spherical structure, having channels, pores and numerous interconnected voids inside explains the chemistry behind drug loading and drug release patterns [41]. They 'cross-link' segments of the DPC to form a porous structure that has many pockets where drugs gets entrapped [24]. The drugs get inclusively complexed into these porous cages. Post administration, over the passing time, the biodegradable cyclodextrin polymer gets slowly degraded to release the entrapped drugs [42].

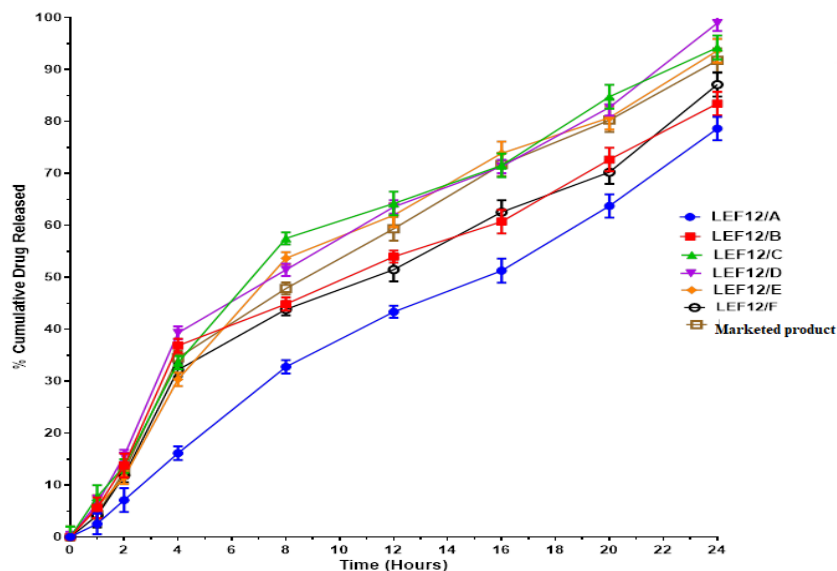


Fig. 17: Drug released profile of entrectinib nanosponges loaded tablets and marketed product, (All determinations were performed in triplicate and values were expressed as mean±SD, n=3)

Drug release kinetics

To elucidate the mode and mechanism of drug release, the data from the *in vitro* release study was applied in different mathematical models and evaluated by correlation coefficient. The highest degree of correlation coefficient determines the suitable mathematical model that follows drug release kinetics [43]. The drug release from the optimized formulation Entrectinib NS loaded tablets follows zero-order kinetics (0.943), which ideal for any drug delivery system. Upon further analysis, the model Korsmeyer-Peppas power law equation states the type of diffusion, which was evaluated by value, n , which is greater than 0.912, which implies that the drug release from the system follow Super case II transport. Case II transport occurs when the sorption is entirely controlled by stress-induced relaxations taking place at a sharp boundary separating an outer swollen shell, essentially at equilibrium penetrant concentration, from an un-penetrated glassy core [44].

CONCLUSION

The Entrectinib-loaded NSs can be formulated by a cost-effective and easy ultrasound-assisted method using hydrophobic polymers such as β -CD. The NS characterization studies confirmed the entrapment of the drug within the colloidal three-dimensional structure of β -CD with the formation of an inclusion complex. The entrapped drugs properties have been modified from crystalline to amorphous nature, which enhances drug solubility. The results of *in vitro* dissolution studies of NS tablets indicated rapid dissolution due to changed solubility properties of the drug, compared to pure drug meeting the set objective enhanced absorption. The formulated Entrectinib-loaded NSs can be beneficial in the treatment of cancers. This can be targeted to the cancer cells and produce sustained drug delivery which in turn reduces the dose, frequency of administration and side effects. The studied are required in future to confirm the anticancer activity of entrectinib-loaded NSs.

FUNDING

Nil

AUTHORS CONTRIBUTIONS

Ms P. Mamatha completed the research work and writing part and Dr. D V R N Bhikshapathi made the correction submission for publication.

CONFLICTS OF INTERESTS

Declared none

REFERENCES

- Weinstein IB, Joe AK. Mechanisms of disease: oncogene addiction-a rationale for molecular targeting in cancer therapy. *Nat Clin Pract Oncol*. 2006 Aug;3(8):448-57. doi: 10.1038/ncononc0558, PMID 16894390.
- Drilon A, Siena S, Ou SI, Patel M, Ahn MJ, Lee J. Safety and antitumor activity of the multitargeted pan-TRK, ROS1, and ALK inhibitor entrectinib: combined results from two phase I trials (ALKA-372-001 and STARTRK-1). *Cancer Discov*. 2017 Apr;7(4):400-9. doi: 10.1158/2159-8290.CD-16-1237, PMID 28183697.
- Meneses Lorente G, Bentley D, Guerini E, Kowalski K, Chow Maneval E, Yu L. Characterization of the pharmacokinetics of entrectinib and its active M5 metabolite in healthy volunteers and patients with solid tumors. *Invest New Drugs*. 2021 Jun;39(3):803-11. doi: 10.1007/s10637-020-01047-5, PMID 33462752.
- Parrott N, Stillhart C, Lindenberg M, Wagner B, Kowalski K, Guerini E. Physiologically based absorption modelling to explore the impact of food and gastric pH changes on the pharmacokinetics of entrectinib. *AAPS J*. 2020 May 26;22(4):78. doi: 10.1208/s12248-020-00463-y, PMID 32458089.
- Meneses Lorente G, Bentley D, Guerini E, Kowalski K, Chow Maneval E, Yu L. Characterization of the pharmacokinetics of entrectinib and its active M5 metabolite in healthy volunteers and patients with solid tumors. *Invest New Drugs*. 2021 Jun;39(3):803-11. doi: 10.1007/s10637-020-01047-5, PMID 33462752.
- Al-Salama ZT, Keam SJ. Entrectinib: first global approval. *Drugs*. 2019 Sep;79(13):1477-83. doi: 10.1007/s40265-019-01177-y, PMID 31372957.
- Sharma M, Sharma R, Jain DK. Nanotechnology-based approaches for enhancing oral bioavailability of poorly water soluble antihypertensive drugs. *Scientifica (Cairo)*. 2016 Apr;2016:8525679. doi: 10.1155/2016/8525679, PMID 27239378.
- Kanugo A, Misra A. New and novel approaches for enhancing the oral absorption and bioavailability of protein and peptides therapeutics. *Ther Deliv*. 2020 Nov;11(11):713-32. doi: 10.4155/tde-2020-0068, PMID 33225869.
- Gupta M. Inorganic nanoparticles: an alternative therapy to combat drug-resistant infections. *Int J Pharm Pharm Sci*. 2021 Aug;13(8):20-31. doi: 10.22159/ijpps.2021v13i8.42643.
- Sarvan, Vashisth H. Types and application of pharmaceutical nanotechnology: a review. *Int J Curr Pharm Sci* 2023;15(3):14-8. doi: 10.22159/ijcpr.2023v15i3.3010.
- Ankem B, Kucharlapati SLT, Magapu SD, BB. Nanosponges-a revolutionary targeted drug delivery nanocarrier: a review. *Asian J Pharm Clin Res*. 2023 Apr;16(4):3-9. doi: 10.22159/ajpcr.2023.v16i4.46453.
- Subair TK, Mohanan J. Development of nano-based film forming gel for prolonged dermal delivery of luliconazole. *Int J Pharm Pharm Sci*. 2022 Feb;14(2):31-41. doi: 10.22159/ijpps.2022v14i2.43253.
- Sharma P, Sharma A, Gupta A. Nanosponges: as a dynamic drug delivery approach for targeted delivery. *Int J App Pharm*. 2023 May;15(3):1-11. doi: 10.22159/ijap.2023v15i3.46976.
- Mendes C, Meirelles GC, Barp CG, Assreuy J, Silva MAS, Ponchel G. Cyclodextrin based nanosponge of norfloxacin: intestinal permeation enhancement and improved antibacterial activity. *Carbohydr Polym*. 2018 Sep 1;195:586-92. doi: 10.1016/j.carbpol.2018.05.011, PMID 29805015.
- Ponnagantimuralikrishna A, Palanati Mamatha. Formulation and optimization of ceritinib loaded nanobubbles by box-behnken design. *Int J Appl Pharm*. 2022 Jul;14(4):219-26.
- Politis SN, Colombo P, Colombo G, Rekkas DM. Design of experiments (DoE) in pharmaceutical development. *Drug Dev Ind Pharm*. 2017 Jun;43(6):889-901. doi: 10.1080/03639045.2017.1291672.
- Konda M, Sampathi S. Qbd approach for the development of capsaicin-loaded stearic acid-grafted chitosan polymeric micelles. *Int J App Pharm*. 2023 Jul;15(4):131-42. doi: 10.22159/ijap.2023v15i4.48101.
- Sharma K, Kadian V, Kumar A, Mahant S, Rao R. Evaluation of solubility, photostability and antioxidant activity of ellagic acid cyclodextrin nanosponges fabricated by melt method and microwave-assisted synthesis. *J Food Sci Technol*. 2022 Mar;59(3):898-908. doi: 10.1007/s13197-021-05085-6, PMID 35153320.
- Aldawsari MF, Alhowail AH, Anwer MK, Ahmed MM. Development of diphenyl carbonate-crosslinked cyclodextrin based nanosponges for oral delivery of baricitinib: formulation, characterization and pharmacokinetic studies. *Int J Nanomedicine*. 2023 Apr;18:2239-51. doi: 10.2147/IJN.S405534, PMID 37139486.
- Anwer MK, Ahmed MM, Aldawsari MF, Iqbal M, Kumar V. Preparation and evaluation of diosmin-loaded diphenyl carbonate-cross-linked cyclodextrin nanosponges for breast cancer therapy. *Pharmaceuticals (Basel)*. 2022 Dec;16(1):19. doi: 10.3390/ph16010019, PMID 36678517.
- Patel M, Sawant K. A quality by design concept on lipid-based nanoformulation containing antipsychotic drug: screening design and optimization using response surface methodology. *J Nanomed Nanotechnol*. 2017 May;08(3):1-11. doi: 10.4172/2157-7439.1000442.
- Rezaei A, Varshosaz J, Fesharaki M, Farhang A, Jafari SM. Improving the solubility and *in vitro* cytotoxicity (anticancer activity) of ferulic acid by loading it into cyclodextrin nanosponges. *Int J Nanomedicine*. 2019 Jun;14:4589-99. doi: 10.2147/IJN.S206350, PMID 31296988.

23. Sherje AP, Dravyakar BR, Kadam D, Jadhav M. Cyclodextrin-based nanosponges: a critical review. *Carbohydr Polym.* 2017;173:37-49. doi: 10.1016/j.carbpol.2017.05.086, PMID 28732878.
24. Moin A, Roohi NKF, Rizvi SMD, Ashraf SA, Siddiqui AJ, Patel M, Ahmed SM, Gowda DV, Adnan M. Design and formulation of polymeric nanosponge tablets with enhanced solubility for combination therapy. *RSC Adv.* 2020 Sep;10(57):34869-84.
25. Khan A. Prediction of quality attributes (mechanical strength, disintegration behavior and drug release) of tablets on the basis of characteristics of granules prepared by high shear wet granulation. *PLOS ONE.* 2021 Dec;16(12):e0261051. doi: 10.1371/journal.pone.0261051, PMID 34882723.
26. Khan I, Lau K, Bnyan R, Houacine C, Roberts M, Isreb A. A facile and novel approach to manufacture paclitaxel-loaded proliposome tablet formulations of micro or nano vesicles for nebulization. *Pharm Res.* 2020 Jun;37(6):116. doi: 10.1007/s11095-020-02840-w, PMID 32488363.
27. Tafere C, Yilma Z, Abrha S, Yehualaw A. Formulation, *in vitro* characterization and optimization of taste-masked orally disintegrating co-trimoxazole tablet by direct compression. *PLOS ONE.* 2021 Mar;16(3):e0246648. doi: 10.1371/journal.pone.0246648, PMID 33725014.
28. Celik B. Risperidone mucoadhesive buccal tablets: formulation design, optimization and evaluation. *Drug Des Devel Ther.* 2017 Nov;11:3355-65. doi: 10.2147/DDDT.S150774, PMID 29225461.
29. Abbasnezhad N, Kebdani M, Shirinbayan M, Champmartin S, Tcharkhtchi A, Kouidri S. Development of a model based on physical mechanisms for the explanation of drug release: application to diclofenac release from polyurethane films. *Polymers (Basel).* 2021 Apr;13(8):1230. doi: 10.3390/polym13081230, PMID 33920267.
30. Kemkar K, SL, Sathiyarayanan A, Mahadik K. 6-shogaol rich ginger oleoresin loaded mixed micelles enhances *in vitro* cytotoxicity on mcf-7 cells and *in vivo* anticancer activity against dal cells. *Int J Pharm Pharm Sci.* 2018 Jan;10(1):160-8. doi: 10.22159/ijpps.2018v10i1.23077.
31. An JY, Yang HS, Park NR, Koo TS, Shin B, Lee EH. Development of polymeric micelles of oleanolic acid and evaluation of their clinical efficacy. *Nanoscale Res Lett.* 2020;15(1):133. doi: 10.1186/s11671-020-03348-3, PMID 32572634.
32. Kovacs A, Berko S, Csanyi E, Csoka I. Development of nanostructured lipid carriers containing salicylic acid for dermal use based on the quality by design method. *Eur J Pharm Sci.* 2017;99:246-57. doi: 10.1016/j.ejps.2016.12.020, PMID 28012940.
33. Tejashri G, Amrita B, Darshana J. Cyclodextrin based nanosponges for pharmaceutical use: a review. *Acta Pharm.* 2013 Sep;63(3):335-58. doi: 10.2478/acph-2013-0021, PMID 24152895.
34. Tiwari K, Bhattacharya S. The ascension of nanosponges as a drug delivery carrier: preparation, characterization, and applications. *J Mater Sci Mater Med.* 2022 Mar;33(3):28. doi: 10.1007/s10856-022-06652-9, PMID 35244808.
35. Utzeri G, Matias PMC, Murtinho D, Valente AJM. Cyclodextrin-based nanosponges: overview and opportunities. *Front Chem.* 2022 Mar;10:859406. doi: 10.3389/fchem.2022.859406, PMID 35402388.
36. Schwarz C, Mehnert W. Freeze-drying of drug-free and drug-loaded solid lipid nanoparticles (SLN). *Int J Pharm.* 1997 Nov;157(2):171-9. doi: 10.1016/s0378-5173(97)00222-6, PMID 10477814.
37. Shaikh MV, Kala M, Nivsarkar M. Formulation and optimization of doxorubicin loaded polymeric nanoparticles using box-behnen design: ex-vivo stability and *in vitro* activity. *Eur J Pharm Sci.* 2017;100:262-72. doi: 10.1016/j.ejps.2017.01.026, PMID 28126560.
38. Wei TK, Manickam S. Response surface methodology, an effective strategy in the optimization of the generation of curcumin-loaded micelles. *Asia-Pacific J Chem Eng.* 2012 Jan;7(S1)Suppl 1:125-33. doi: 10.1002/apj.661.
39. Danaei M, Dehghankhold M, Ataei S, Hasanzadeh Davarani F, Javanmard R, Dokhani A. Impact of particle size and polydispersity index on the clinical applications of lipidic nanocarrier systems. *Pharmaceutics.* 2018 May;10(2):57. doi: 10.3390/pharmaceutics10020057, PMID 29783687.
40. Abbas G, Hanif M, Khan MA. pH responsive alginate polymeric rafts for controlled drug release by using box behnen response surface design. *Des Monomers Polym.* 2017 Sep;20(1):1-9. doi: 10.1080/15685551.2016.1231046, PMID 29491774.
41. Sharma RK, Yassin AE. Nanostructure-based platforms-current prospective in ophthalmic drug delivery. *Indian J Ophthalmol.* 2014 Jul;62(7):768-72. doi: 10.4103/0301-4738.138301, PMID 25116766.
42. Torne SJ, Ansari KA, Vavia PR, Trotta F, Cavalli R. Enhanced oral paclitaxel bioavailability after administration of paclitaxel-loaded nanosponges. *Drug Deliv.* 2010 Aug;17(6):419-25. doi: 10.3109/10717541003777233, PMID 20429848.
43. Kovacs A, Berko S, Csanyi E, Csoka I. Development of nanostructured lipid carriers containing salicylic acid for dermal use based on the quality by design method. *Eur J Pharm Sci.* 2017;99:246-57. doi: 10.1016/j.ejps.2016.12.020, PMID 28012940.
44. Tardy BL, Mattos BD, Otoni CG, Beaumont M, Majoinen J, Kamarainen T. Deconstruction and reassembly of renewable polymers and biocolloids into next generation structured materials. *Chem Rev.* 2021 Nov;121(22):14088-188. doi: 10.1021/acs.chemrev.0c01333, PMID 34415732.
45. Sengupta P, Chatterjee B, Tekade RK. Current regulatory requirements and practical approaches for stability analysis of pharmaceutical products: a comprehensive review. *Int J Pharm.* 2018;543(1-2):328-44. doi: 10.1016/j.ijpharm.2018.04.007, PMID 29635054.